Submitted to the Editor of the Astrophysical Journal *Letter* date

Three New Supernova Remnant OH Masers Near the Galactic Center: Evidence for Large Scale Maser Emission from Supernova Remnants

F. Yusef-Zadeh

Department of Physics and Astronomy, Northwestern University, Evanston, Il. 60208

(zadeh@nwu.edu)

W. M. Goss

National Radio Astronomy Observatory, P.O. Box 0, Socorro, New Mexico 87801

(mgoss@nrao.edu)

D. A. Roberts

University of Illinois, 1002 Green St., Urbana, IL 61801 (dougr@ncsa.uiuc.edu)

B. Robinson

Department of Physics and Astronomy, Northwestern University, Evanston, Il. 60208

D. A. Frail

National Radio Astronomy Observatory, P.O. Box 0, Socorro, New Mexico 87801

(dfrail@aoc.nrao.edu)

Received 00 ; accepted 00

ABSTRACT

A survey of the inner $8^\circ \times 1^\circ$ of the Galactic plane toward the Galactic center has been carried out at the 1720 MHz transition of OH molecule using the VLA in its D configuration with a resolution of $\approx 70'' \times 45''$. The detection of compact 1720 MHz OH masers associated with three supernova remnants G357.7+0.3, G1.13–0.1 (Sgr D) and G1.4–0.1 as well as new extended maser line emission from G357.7+0.3 and G357.7–0.1 (the Tornado Nebula) were then followed up by A-array observations with spectral and spatial resolutions of 0.3 $\mathrm{km\,s^{-1}}$ and $\approx 3'' \times 2''$, respectively.

The 1720 MHz OH maser line emission is considered to be a powerful shock diagnostic and is collisionally pumped by H_2 molecules at the site where C-type supernova shocks drive into adjacent molecular clouds. The new observations show clear evidence of extended features coincident with compact and bright masers, the best example of which is a coherent feature over a scale of about 20 pc surrounding the shell of the SNR G357.7+0.3. We argue that this remarkable feature is an OH maser and is physically associated with the remnant. This implies that the ambient molecular cloud is uniform in its density and temperature with restricted range of pumping conditions and survives the passage of a large-scale shock front.

Subject headings: Galaxy: center —ISM: molecules – supernova remnants – magnetic fields, masers – shock waves

1. Introduction

A series of papers have recently examined the interaction site of supernova remnants (SNR's) with molecular clouds, almost two decades after the initial discovery of OH(1720 MHz) maser emission toward supernova remnants (SNRs) by Goss & Robinson (1968). These so-called "supernova remnant masers" (Fukui 1995) signal perhaps the best evidence for the site of physical interaction between molecular clouds and SNRs. In particular, the masers signify shocked gas as the expanding remnant runs into the nearby molecular cloud (Elitzur 1976; Lockett, Gauthier & Elitzur 1998; Wardle, Yusef-Zadeh & Geballe 1998). In addition, the study of OH(1720 MHz) masers in the Galactic center region have provided the estimates of the line of sight magnetic field behind a shock front, the size and shape of scatter-broadened sources masked by the turbulent screen, the length scale of the magnetic fluctuations in the scattering medium and the magnitude of the tidal shear experienced by an expanding nonthermal shell into a dense molecular cloud (Yusef-Zadeh et al. 1999).

The revival of OH(1720 MHz) maser study was initiated by the association of 26 OH(1720) masers with W28, a well known SNR interacting with an adjacent molecular cloud (Frail, Goss & Slysh 1994). Following the survey of well-known SNRs in the disk of the Galaxy (Frail et al. 1996; Green et al 1997; Koralesky et al. 1998), we searched for these masers in the central degree of the Galactic center where two nonthermal sources Sgr A East and G359.1–0.5 showed association with OH(1720 MHz) masers (Yusef-Zadeh et al. 1995, 1996). Using the Very Large Array of the National Radio Astronomy Observatory[1] the present survey covers an expanded area near the Galactic center; we report the detection of three new SNR masers (G357.7+0.3, G1.05-0.15 and G1.4-0.1 as seen in Figure 1) within the inner few degrees of the Galactic center. We also report the detection of extended OH

[1]The National Radio Astronomy Observatory is a facility of the National Science Foundation, operated under a cooperative agreement by Associated Universities, Inc.

maser emission associated with G357.7+0.3 and G357.7–0.1 (the Tornado Nebula). The latter source was known to have an associated compact OH maser emission (Frail et al. 1996).

2. Observations

The OH 1720 MHz maser line observations were made on 19 and 28 August 1996, using the compact D configuration of the VLA. A total of 88 antenna pointings were used covering roughly the inner $8^\circ \times 1^\circ$ ($l \times b$) of the Galactic center region. Figure 1 shows a sketch of 85 circles, each of which represents the $26'$ FWHM of the primary beam. The filled circles in this figure show the positions where new OH(1720 MHz) masers have been detected. Figure 1 also shows three additional filled circles associated with the Galactic center, Sgr A, G359.5–0.18 and W28; in these cases supernova maser emission had been reported previously (Yusef-Zadeh, Uchida & Roberts 1995; Frail, Goss & Slysh 1994; Yusef-Zadeh et al. 1996, 1999). Roughly 5 minutes were spent observing each field using the four IF mode of the VLA correlator in two overlapping spectral windows. Each IF pair simultaneously observed right and left circular polarization in 127 channels with a total bandwidth of 1.5625 MHz (273 $\mathrm{km\,s^{-1}}$). In order to maximize a total velocity coverage, the two IF pairs were centered at $V_{\mathrm{LSR}} = -80$ and $+80$ $\mathrm{km\,s^{-1}}$, respectively.

The calibration of the absolute flux density, the complex gains, and the bandpass response was carried out with the Astronomical Image Processing System (AIPS) of the NRAO. The data from the two IF pairs covered a total velocity range of ± 216 $\mathrm{km\,s^{-1}}$. Data from the line-free channels were used to remove the continuum from the line data in the visibility plane with the AIPS task UVLSF. Final imaging, image processing, visualization, and profile analysis were carried out with the Multichannel Image Reconstruction, Image Analysis and Display (MIRIAD) system of the Berkeley-Illinois-Maryland Association

(BIMA). The images were made with natural weighting for optimal sensitivity with beam size of $\approx 70'' \times 45''$ image and Hanning smoothed off-line to give a velocity resolution of 4.25 $\mathrm{km\,s^{-1}}$.

Follow-up high-resolution observations were carried out on November 22 and December 24, 1996 in the A-array configuration of the VLA in order to improve the spatial and velocity structure of the masers initially found in the low-resolution D array observations. We observed four fields centered on G357.7+0.3 (α, δ[1950] = $17^{\rm h}35^{\rm m}\ 17\overset{\rm s}{.}7$, $-30^\circ 32' 01''$ at $V_{\rm LSR}$=–35 $\mathrm{km\,s^{-1}}$), G357.7–0.1 ($17^{\rm h}36^{\rm m}\ 54\overset{\rm s}{.}3$, $-30^\circ 56'\ 15\overset{''}{.}0$ at $V_{\rm LSR}$=–5 $\mathrm{km\,s^{-1}}$), Sgr D ($17^{\rm h}45^{\rm m}\ 43\overset{\rm s}{.}0$, $-28^\circ 10'\ 25\overset{''}{.}0$ at $V_{\rm LSR}$=–5 $\mathrm{km\,s^{-1}}$) and G1.4–0.1 ($17^{\rm h}46^{\rm m}\ 19\overset{\rm s}{.}2$, $-27^\circ 46'\ 52\overset{''}{.}0$ at $V_{\rm LSR}$=–3 $\mathrm{km\,s^{-1}}$) in the 1720 MHz hyperfine transition of OH molecule. Using both the right (RCP) and left (LCP) hands of circular polarization, the 195.3 kHz bandwidth and 127 channels gave a velocity resolution of 0.27 $\mathrm{km\,s^{-1}}$ after online Hanning smoothing. The final images had typical synthesized beam of $2\overset{''}{.}5 \times 1\overset{''}{.}3$ (PA=$3\overset{\circ}{.}9$) and typical rms noise of $\approx$12 mJy $\mathrm{beam^{-1}}$ per channel. Images of Stokes V and I based on A array observations were also made for the three new sources. The upper limits to their line-of-sight magnetic field via the Zeeman effect are measured. The polarization data indicate 3-σ upper limits of 1.7, 2.2, 1.7, 0.6, 0.5 mG for G1.4–0.1, G357.7–0.1, G357.7+0.3 OH1720:A1, A2, A5 (see Table 1).

3. Results

The D array survey showed three new sources of maser emission associated with nonthermal radio continuum sources. A new extended OH(1720 MHz) emission is also detected toward the Tornado nebula, as described below. Table 1 lists the Gaussian fitted position and velocity of the compact sources as well as their deconvolved sizes based on A array observations. The errors to the positions depend on signal-to-noise ratio.

3.1. G357.7+0.3 (The Square Nebula)

The continuum source G357.7+0.3 is a probable SNR (Reich & Fürst 1984; Leahy 1989; Gray 1994); the radio source is linearly polarized and has a steep spectral index, with a shell-like appearance and its associated X-ray emission. The structure of this unusual continuum source is noted for its nearly square-like morphology (Gray 1994). There is also an appearance of distorted structure to the NW of the continuum feature. Figure 2 shows the grayscale continuum image of the source with a spatial resolution of $83'' \times 43''$ based on Mologolo Observatory Synthesis Telescope (MOST) observations at 843 MHz made by Gray (1994). Superposed on this image are naturally weighted contour image of maser emission averaged between –42 and –29 $\mathrm{km\,s^{-1}}$ with a resolution of $100'' \times 100''$ based on the D array data. We note that the contours of OH(1720 MHz) emission mimic closely the shape of the continuum structure to the NW of the continuum image. In this region the extended OH(1720 MHz) structure is seen on a scale of $15'$. Since the phase center of the VLA observations was placed to the NW of G357.7+0.3, (at $\alpha(1950) = 17^{\mathrm{h}}35^{\mathrm{m}}17.8^{\mathrm{s}}, \delta(1950) = -30^{\circ}32'01''$) the best sensitivity to detecting the line emission lies in this region of the remnant. The contours shown to the SW may have been affected by the primary beam correction, which amplifies the noise at the edge of the primary beam. However, it is clear that the OH(1720 MHz) line feature is quite large, the $15'$ extent outlines the eastern half of this unusual nonthermal feature. The large-scale OH feature is noted best at a velocity of –35.4 $\mathrm{km\,s^{-1}}$where an evelope of weak emission with a flux density of ≈20 mJy/beam is distributed on a a scale of $15'$; Several bright sources on the scale of the beam which is $86'' \times 45.7''$ are surrounded by the large scale OH feature. Most of the extended emission was resolved out in high resolution data implying that the emission is diffuse. The peak diffuse emission is 127 mJy/beam with the beam size of $69'' \times 34''$ (at $\alpha(1950) = 17^{\mathrm{h}}35^{\mathrm{m}}17.78^{\mathrm{s}}, \delta(1950) = -30^{\circ}31'21''$) should have been detected in the A array images with a sensitivity of 52 mJy/beam if the emission were collection of

point sources. It is noteworthy that the strongest maser emission near –35 $\mathrm{km\,s^{-1}}$ coincides with the NW region of the remnant where the continuum distribution shows a prominant departure from circular-shaped geometry.

Table 1 lists the peak positions and central velocities of five sources (A1 – A5) seen in the A array image. The bright peak emission in low-resolution data, as shown in the contours of Figure 2, breaks up into five sources in the A array observations. The crosses on this figure represent the position of compact sources seen in the A-array observations. Although much of the extended features seen in Figure 2 are resolved out in the A array images, the extended emission with the resolution of $3\farcs2 \times 1\farcs5$ at a level of $\sim$ 5 to 25 mJy $\mathrm{beam^{-1}}$ corresponding to $T_b \approx$ 530 to 2600 K is detected between the compact and bright maser sources listed in Table 1. We also note that source A3 has a size of $\approx 4.9'' \times 2.5''$ with a position angle of 42^0. This position clearly shows that the compact features are also resolved along the direction of the SNR shell. The peak flux density of the compact sources is ≈500 mJy $\mathrm{beam^{-1}}$ which correspond to $T_b \approx 5 \times 10^4$ K. Two spectra showing the extended emission observed both in the D and A array data are shown in Figure 3. The D array emission spectrum (left) which arises from the position $\alpha(1950) = 17^{\mathrm{h}}35^{\mathrm{m}}07^{\mathrm{s}}, \delta(1950) = -30^\circ 32' 41''$ is not detected due to its large size of more than $2'$ in the A array data whereas the A-array spectrum (right) arises from a diffuse region of size $5'' \times 7''$ near $\alpha(1950) = 17^{\mathrm{h}}35^{\mathrm{m}}17.8^{\mathrm{s}}, \delta(1950) = -30^\circ 32' 16.5''$. The extended components show similar kinematics as the compact components at velocities near –35 $\mathrm{km\,s^{-1}}$.

3.2. G357.7–0.1 (the Tornado Nebula)

This elongated radio continuum source called the Tornado nebula is known to have a nonthermal origin with a spectral index consistent with a shell-type SNR estimated to be

located at a distance greater than 6 kpc (Radhakrishnan et al. 1972; Shaver et al. 1985a; Helfand & Becker 1985; Stewart, et al. 1994). The compact source at the western edge of G357.7–0.1 is considered to be an HII region based on its IRAS spectrum and ^{12}CO emission at +9 km s^{-1} (Shaver et al. 1985b; see an alternative interpretation by Shull, Fesen & Shaken 1989). Frail et al. (1996) detected an OH(1720 MHz) maser source at the western edge of the Tornado (beam of $\approx 15''$) and to the north of the bright compact continuum source at a velocity of –12.4 km s^{-1} with a peak flux density of 277 mJy.

The A array observations with a resolution of $3\farcs2 \times 1\farcs5$ detect this maser spot with a position in good agreement with Frail et al. (1996). Table 1 lists the properties of the resolved maser spot with a flux density of 209 mJy at the velocity of –12.2 km s^{-1}. The low-resolution observations show the compact maser spot as well as a newly detected extended OH(1720 MHz) structure to the northeast of the nonthermal feature. The extended structure is best seen in Figure 4 where the contours represent the line emission averaged between –13.1 and –8.7 km s^{-1} with a spatial resolution of $114'' \times 38''$ based on the D array data. The high-resolution grayscale continuum image of the Tornado nebula (Shaver et al. 1985a) is also shown. The cross represents the position of the maser spot detected in A array observations. The extended line emitting feature is observed at a velocity close to the velocity of the compact source coinciding with the brightest continuum feature. The extended line emission is weak with a typical flux density ranging between 25 and 40 mJy beam^{-1} (rms noise 2.5 mJy beam^{-1}). The morphology and the kinematics of OH(1720 MHz) features as well as their brightness temperatures suggest that the compact and extended structures are masers and are associated with the nebula (see section 4).

3.3. Sgr D & G1.4–0.1

Sgr D is a bright radio continuum source near the Galactic center. Sgr D consists of two adjacent radio continuum sources. One of the sources G1.13–0.10 is an HII region coinciding with a star forming region and the other is SNR G1.05–0.15 with nonthermal characteristics which is considered to be located near or beyond the Galactic center (Downes et al. 1979; Odenwald & Fazio 1984; Liszt 1992; Gray 1994; Mehringer et al. 1998).

Figure 5 taken from the continuum survey by Liszt (1992), shows a mosaic continuum image of the Sgr D region located in the bottom half of the figure with a spatial resolution of $30'' \times 15''$ PA=0^0. The two bright continuum sources G1.13–0.10 and G1.05–0.15 are observed adjacent to each other near $\alpha(1950) = 17^{\rm h}45^{\rm m}20^{\rm s}, \delta(1950) = -28^\circ05'$. The weak shell-like structure G1.4–0.1 (to the north) about $15'$ NW of the Sgr D region (Liszt 1992; Mehringer et al. 1998).

Our low-resolution OH survey observations showed two compact maser spots toward G1.4–0.1 and G1.05–0.15 at velocities of –2.5 and –1.4 $\rm km s^{-1}$, respectively. The low-resolution peak of G1.4–0.1 consists of two components whereas the maser spot in G1.05–0.15 is unresolved in the A array observations. These compact OH(1720 MHz) maser spots associated with nonthermal sources are represented by a crosses in Figure 4. The properties of these maser spots are described in Table 1. We also noted extended thermal emission toward the thermal component of the Sgr D region in the D array data. Contours in this figure represent OH(1720 MHz) emission at a velocity of -16.2 $\rm km s^{-1}$ based on D array observations.

4. Discussion

The common OH masers at 1665, 1667, and 1612 MHz are generally associated with HII regions and evolved stars and are thought to be pumped by far-IR radiation. The class of OH(1720 MHz) masers is distinguished from traditional OH masers by being spatially and kinematically associated with SNRs, shows none of the other transitions of OH and is probably pumped collisionally. Recent theoretical and observational studies suggest that the OH(1720 MHz) masers are associated with C-type shocks and are collisionally pumped in molecular clouds at temperatures and densities 50 – 125 K and $10^5 - 10^6$ cm^{-3} (Lockett et al. 1999; Wardle et al. 1998; Frail and Mitchell 1998). The evidence for C-type shocks is also suggested by infrared emission lines of H_2O and OH from a number of interacting SNRs with molecular clouds (Reach and Rho 1998a, 1998b). In a recent model, Wardle et al. (1998) argue that the X-ray photodissociation in SNR masers is responsible for enhancing the OH abundance behind the C-type shock fronts. The evidence for the association of a number of composite SNRs (i.e. center-filled morphology in X-rays and shell-like morphology in radio continuum) and SNR masers including G357.7+0.3 is consistent with this suggested model.

Another distinction that may characterize traditional OH masers and SNR OH masers is their linear sizes. We note the presence of a remarkable extended OH(1720 MHz) feature in G357.7+0.3 distributed over an angular size of 15′ corresponding to 27 pc at the distance of 6.4 kpc (Leahy 1989). Such an extended coherent structure which has been observed in at least three other supernova maser sources (G359.1–0.5, 3C391 and Tornado), is argued below to have maser characteristics. This association provides additional support to the large-scale nature of the interaction of the SNR with adjacent molecular clouds.

What is the nature of spatially extended OH(1720 MHz) emission? One possibility is that these prominent extended features are due to slightly enhanced excitation temperature

of thermal foreground objects having a similar origin to widespread Galactic OH(1720 MHz) emission observed in the Galactic plane using single dish telescopes (Haynes and Caswell 1977; Turner 1982). Alternatively, these features could be low-gain masers and co-exist with compact masers as has been argued in the case of G359.1-0.5 (Yusef-Zadeh, Uchida and Roberts 1995).

Based on the spectra shown in Figure 3, we believe that the emitting extended OH features observed in both the D and A array images of G357.7+0.3 are associated with the compact OH(1720 MHz) maser spots having high brightness temperatures. First, both the extended OH features coincide with the radio continuum edges. However, both the compact and extended OH(1720 MHz) features show no clear correlation with the strength of background radio continuum emission from the SNRs. In the case of widely spread OH(1720 MHz) masers, strong background radio sources either from thermal or nonthermal continuum radio sources are required. The extended OH(1720 MHz) features show a range of brightness temperatures between 10 and 2500 K on scales varying from several arcseconds to several arc minutes; no 1720 MHz absorption lines have been detected toward this source. The brightness temperature of the extended emitting features at some locations is much greater than the gas temperature. Also, the brightness temperature of the line emission is much less than the the brightness temperature of the continuum emission. The lack of detecting any observed OH (1720 MHz) absorption lines argues against a thermal origin of the optically thin extended OH features. In the 88 D array search positions in the Galactic center, extended OH (1720 MHz) emission is detected in four regions with compact 1720 MHz maser spots. This coincidence suggets that the extended and compact OH (1720 MHz) sources are physically associated.

Second, the compact source A3 in G357.7+0.3, (see Table 1, size 3.5″) is oriented along the direction of the nonthermal shell in agreement with the large-scale extended

OH structures. The largest size of the scatter-broadened OH(1720 MHz) maser sources associated with Sgr A East at the Galactic center is only 1.3″ (Yusef-Zadeh et al. 1999). It is unlikely that the size of source A3 can be explained by scatter broadening; Unless G357.7+0.3 lies behind an extended HII region, the resolved sizes of OH sources given in Table 1 are likely to be due to intrinsically extended nature of OH(1720 MHz) maser emission. Furthermore, the narrow line widths of a few $\mathrm{km\,s^{-1}}$ for the extended features are similar to the compact sources; these line widths are an order of magnitude less than the linewidth of molecular clouds in the Galactic center region (Bally *et al.* 1988). The kinematics and the location of the compact and extended features suggest that they are located at the boundary of a –35 $\mathrm{km\,s^{-1}}$ molecular cloud and the G357.7+0.3 nonthermal shell source.

The remarkable similarity in the shape of the large-scale extended OH(1720 MHz) emission and the nonthermal continuum distributions implies that the system of SNR-molecular clouds are interacting. Another signature of the physical interaction between SNRs and molecular clouds may be the highly distorted appearance of the remnants (e.g. G357.7+0.1 and the Tornado nebula G357.7–0.1). G357.7+0.3 has a square-shape geometry and the region to its NW appears to be most distorted (see the original figure by Gray 1994). There are no known molecular observations of the ambient gas in the vicinity of G357.7+0.3, the extended OH(1720 MHz) emission may well suggest the existence of an extended molecular cloud surrounding G357.7+0.3. The fact that the SNR deviates from a shell-like geometry at the interaction site may suggest the following picture: The pressure of X-ray gas in the interior of the expanding shell may not be sufficient to dominate the magnetic field pressure behind the shock front leading to a distortion of the shell-like structure of the remnant as it collides with the dense molecular cloud. Future Zeeman measurements of the extended OH(1720 MHz) masers as well as molecular line observations have the potential to quantify the physical conditions of the shocked gas and the ambient

cloud as well as to determine the scale lengths over which the magnetic field are organized behind the large-scale shocks.

It is possible that large-scale OH(1720 MHz) maser emission is a distinct character of these types of masers. The cloud must be relatively homogeneous in its gas temperature and density in order for OH(1720 MHz) maser to be pumped collisionally on such a scale under the restricted conditions. Unlike traditional OH masers, these large-scale OH(1720 MHz) masers point to a global low-gain population inversion of OH in the extended ambient cloud caused by the passage of a shock front. The present data are ambiguous in distinguishing whether the variations of the brightness temperature, as seen in Figure 2, results from gas temperature or gas density variations. The compact maser sources arise along the edge of the supernova shells where the acceleration is considered to be perpendicular to the line of sight and where the velocity coherence is achieved with a small velocity gradient along the line of sight. For large-scale maser sources, the acceleration is unlikely to be perpendicular to the line of sight throughout a latge region of the cloud, thus resulting a velocity difference between the compact and extended sources (e.g. 3C391).

In conclusion, we have searched for signs of physical interaction between nonthermal radio continuum sources and molecular clouds in the Galactic center region by using the OH(1720 MHz) maser emission as a probe. Three new masers which are all associated with SNRs have been discovered in this survey. These detections plus three SNR masers from previous measurements bring a total of six SNR masers found among 17 searched SNRs (Green 1998) toward the Galactic center region. Although the sample of searched SNRs is incomplete, the high detection rate of 35% in the longitudes between -4.5^0 and 5.5^0 is more than three times the rate of detection found elsewhere in the disk of the Galaxy (e.g. Green et al. 1997). This high rate of detection may be explained by high density of molecular gas distributed throughout the inner few degrees of the Galactic center, thus providing the

physical conditions required to produce OH(1720 MHz) emission.

Acknowledgments: We thank W. Cotton, A. Gray and C. Salter for providing continuum images and Mark Wardle for useful discussions.

REFERENCES

Bally, J., Stark, A.A., Wilson, R.W., & Henkel, C. 1988, ApJ, 324, 223

Claussen, M.J., Frail, D.A., Goss, W.M., & Gaume, R.A. 1997, ApJ 489, 143

Downes, D., Wilson, T., Bieging, J., & Wink, O. 1980, A&AS, 35, 1

Elitzur, M. 1976, ApJ, 203, 124

Frail, D.A. & Mitchell, G.F. 1998, ApJ, 508, 690.

Frail, D.A., Diamond, P.J., Cordes, J.M. & van Langevelde, H.J. 1994, ApJ, 427, L43

Frail, D. A., Goss, W. M., Reynoso, E. M., Giacani, E.B., Green, A. J. & Otrupcek, R. 1996, AJ, 111, 1651

Frail, D.A., Goss, M.W. & Slysh, V.I. 1994, ApJ, 424, L111

Fukui, Y. 1995, Science 270, 1771

Goss, W.M. & Robinson, B.J. 1968, ApJ, 2, L81

Gray, A.D. 1994, MNRAS, 270, 835

Green, D.A. 1998, A catalogue of Galactic Supernova Remnants (1998 September version), Mullard Radio Astronomy Observatory Cambridge, UK (http://www.mrao.cam.ac.uk/surveys/snrs/)

Green A.J., Frail, D.A., Goss, W.M. & Otrupcek, R. 1997, AJ, 114, 2058

Haynes, R.F. & Caswell J.L. 1977, MNRAS, 178, 219

Helfand, D.J. & Backer, R.H. 1985, Nature, 313, 118

Koralesky, B., Frail, D.A., Goss, W.M., Claussen, M.J. & Green, A.J. 1998, AJ, 116, 1323

Leahy, D.A. 1989, ApJ, 216, 193

Liszt, H.S. 1992, ApJS, 82, 495

Lockett, P., Gauthier, E. & Elitzur, M. 1998, ApJ, 511, 235

Mehringer, D.M., Goss, W.M., Lis, D.C., Palmer, P. & Menten, K.M. 1998, ApJ, 493, 274

Odenwald, S.F. & Fazio, G.G, 1984, ApJ, 283, 601

Reach, W.T. & Rho, J. 1998a, ApJ, 507, L93

Reach, W.T. & Rho, J. 1998b, ApJ, 511, 836

Radhakrishnan, V., Goss, W.M., Murray, J.D. & Brooks, J.W. 1972, ApJS, 24, 49

Reich, W. & Fürst, E. 1984, A&AS, 57, 165

Shaver, P.A., Salter, C.J., Patnaik, A.R., van Gorkom, J.H. & Hunt, G.C. 1985a, Nature, 313, 113

Shaver, P.A., Pottash, S.R., Salter, C.J., Patnaik, A.R., van Gorkom, J.H. & Hunt, G.C. 1985b, A&A, 147, L23

Stewart, R.T., Haynes, R.F. Gray, A.D. & Reich, W. 1994, ApJ, L39

Wardle, M., Yusef-Zadeh, F., & Geballe 1998, preprint (astro-ph 9811090).

Yusef-Zadeh, F., Uchida, K.I., & Roberts, D.A. 1995, Science 270, 1801

Yusef-Zadeh, F., Roberts, D.A., Goss, W.M., Frail, D.A. & Green, A. 1996, ApJ 466, L25

Yusef-Zadeh, F., Roberts, D.A., Goss, W.M., Frail, D.A. & Green, A. 1999, ApJ, 512, 230.

This manuscript was prepared with the AAS LaTeX macros v4.0.

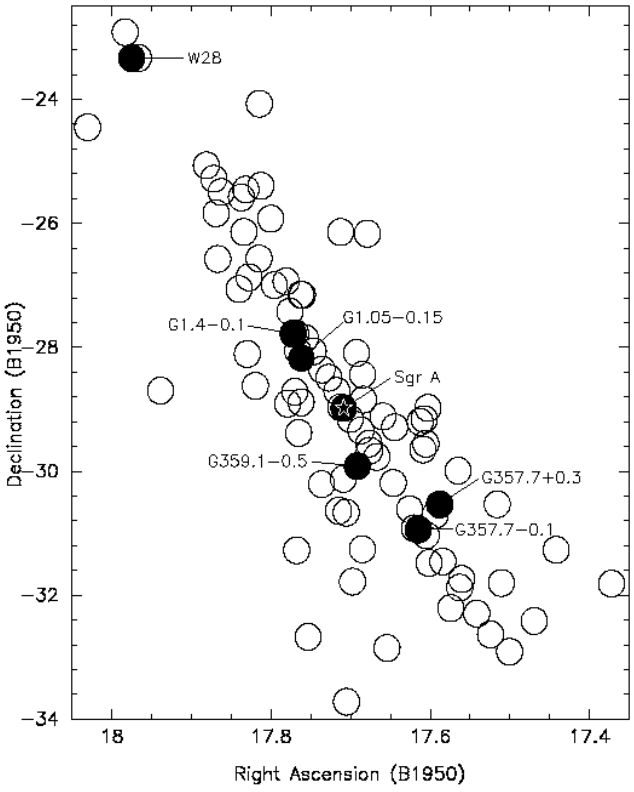

Fig. 1.— A representation of the area searched in the 88 pointings of the D-array 1720 MHz OH observations along the Galactic plane near the Galactic center. The size of each circle (26′ diameter) corresponds to the full width at half maximum of the primary beam at 1720 MHz. The filled circles coincide with regions where OH(1720 MHz) masers associated with SNRs have been detected from this and previous observations. The star symbol corresponds to the position of Sgr A* at the Galactic center.

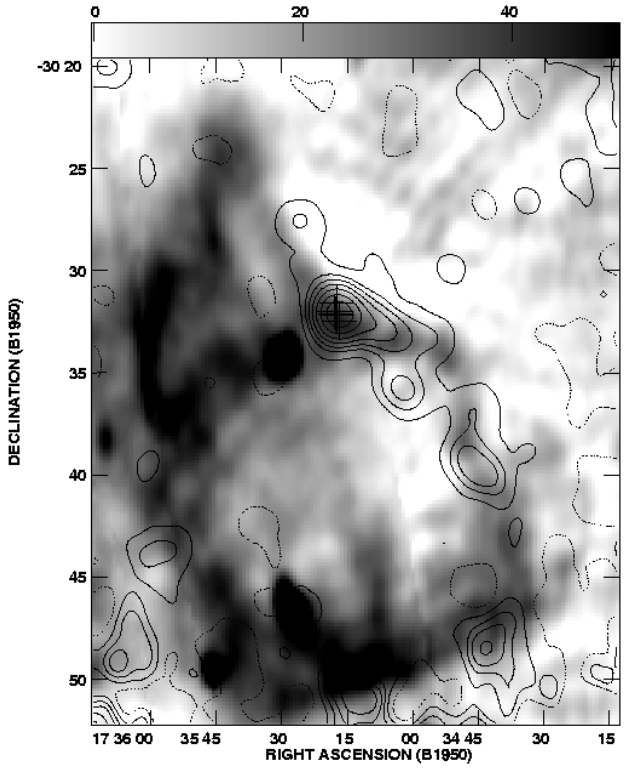

Fig. 2.— A grey-scale continuum image of G357.7+0.3 shown in black with a resolution of $83'' \times 43''$ (Gray 1994) superimposed on the contours of velocity averaged OH(1720 MHz) emission between –42 and –29 $\mathrm{km\,s^{-1}}$ convolved with beam of $100'' \times 100''$ having an rms noise of 3.2 mJy $\mathrm{beam^{-1}}$. The levels are 32.5 × (–3, 3, 8, 13, 20, 30, 45, 65) mJy $\mathrm{beam^{-1}}$ $\mathrm{km\,s^{-1}}$. The crosses at the peak contour position corresponds to the position of maser spots detected in the A array observations with a resolution of $2\farcs8 \times 1\farcs4$.

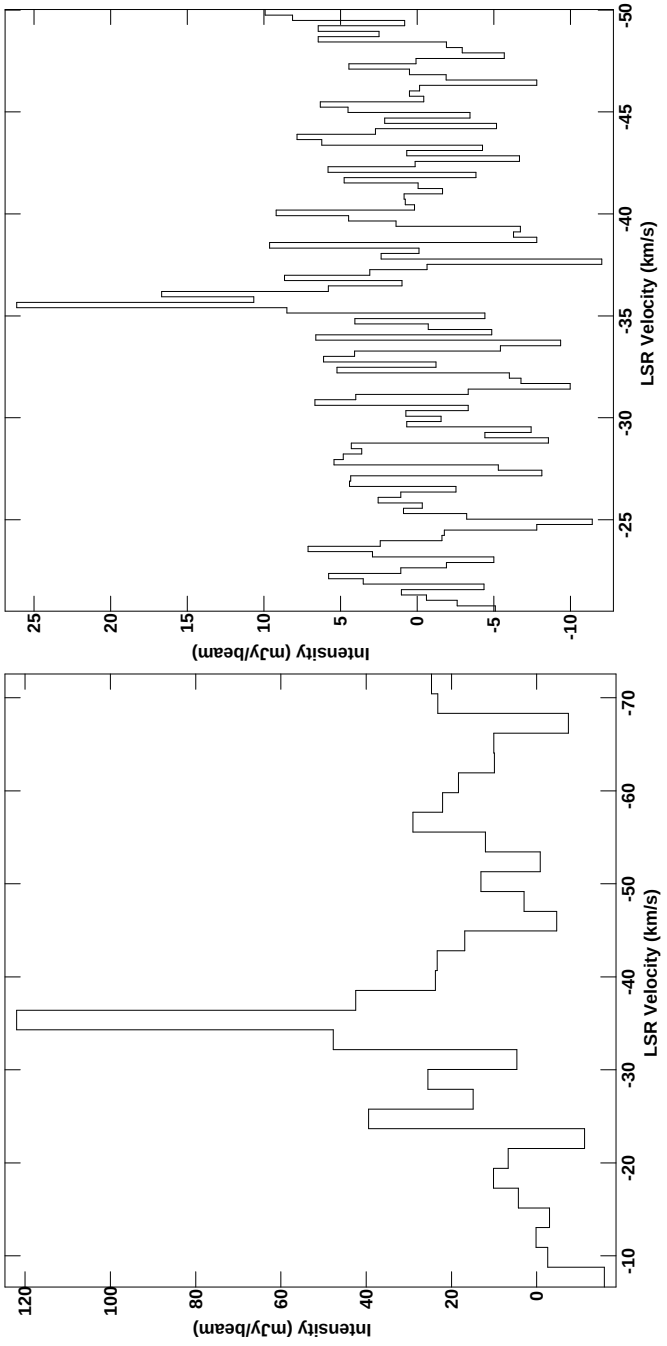

Fig. 3.— Two Stokes I spectra from the diffuse regions of G357.7+0.3 based on the D array data (left) with a spatial resolution of $69'' \times 34''$ and the A array data (right) with a resolution of $2\farcs8 \times 1\farcs4$. The left panel centered at $\alpha(1950) = 17^{\rm h}35^{\rm m}07^{\rm s}, \delta(1950) = -30°32'41''$ whereas the right spectrum is integrated over a $5'' \times 7''$ region centered on $\alpha(1950) = 17^{\rm h}35^{\rm m}17.8^{\rm s}, \delta(1950) = -30°32'16.5''$

.

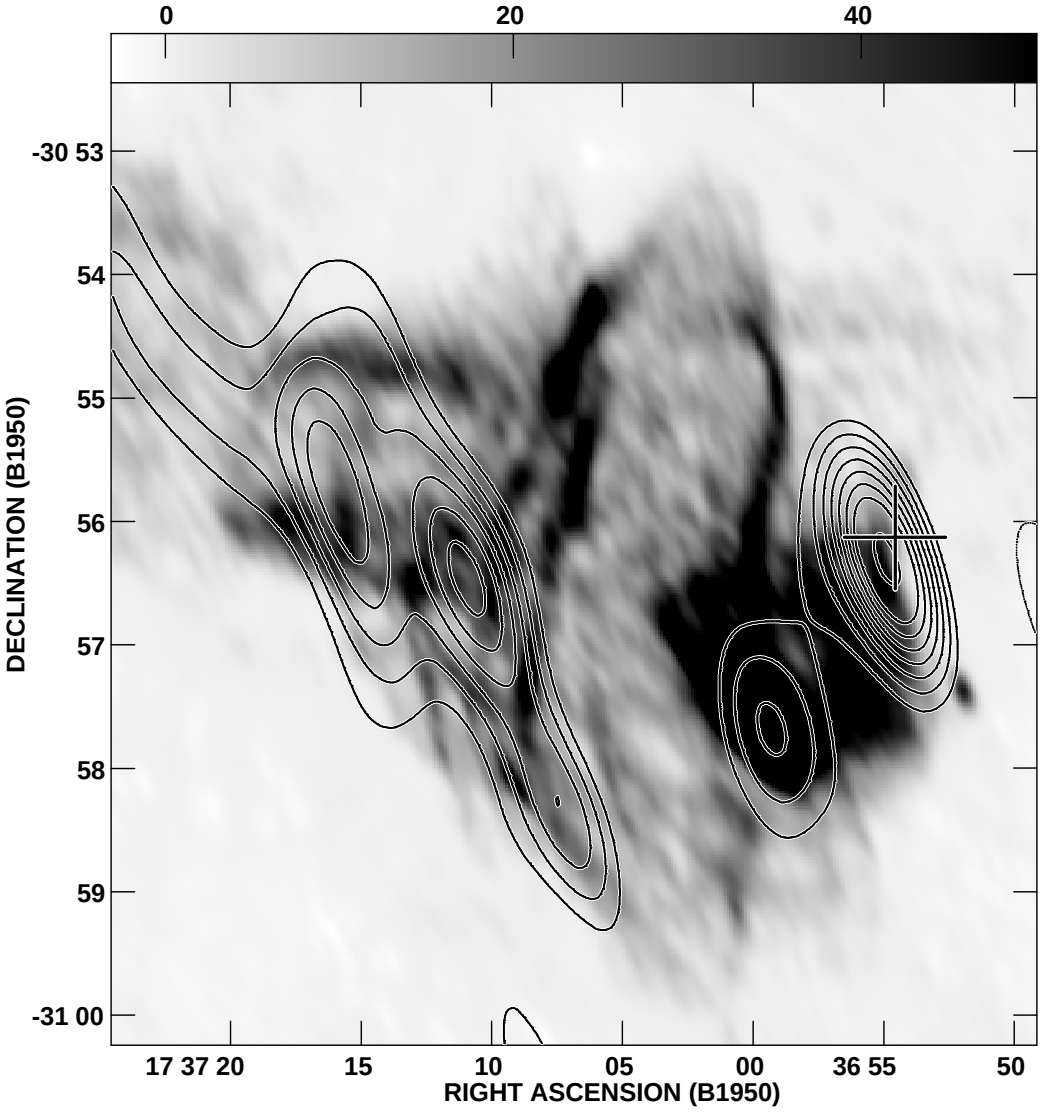

Fig. 4.— A grey-scale continuum image of G357.7–0.1 shown in black with a resolution of $14.6'' \times 4.9''$ provided by C. Salter with contours of velocity averaged OH(1720 MHz) emission between –13.1 and –8.7 $\mathrm{km s^{-1}}$ at a spatial resolution of $114'' \times 38''$ (PA=20^0) superposed. The levels are 22 × (–3, 3, 4, 5, 6, 7, 8, 9, 11, 13, 15) mJy $\mathrm{beam^{-1} km s^{-1}}$. The cross corresponds to the position of the 1720 MHz maser spot observed with a resolution of $3\farcs2 \times 1\farcs5$.

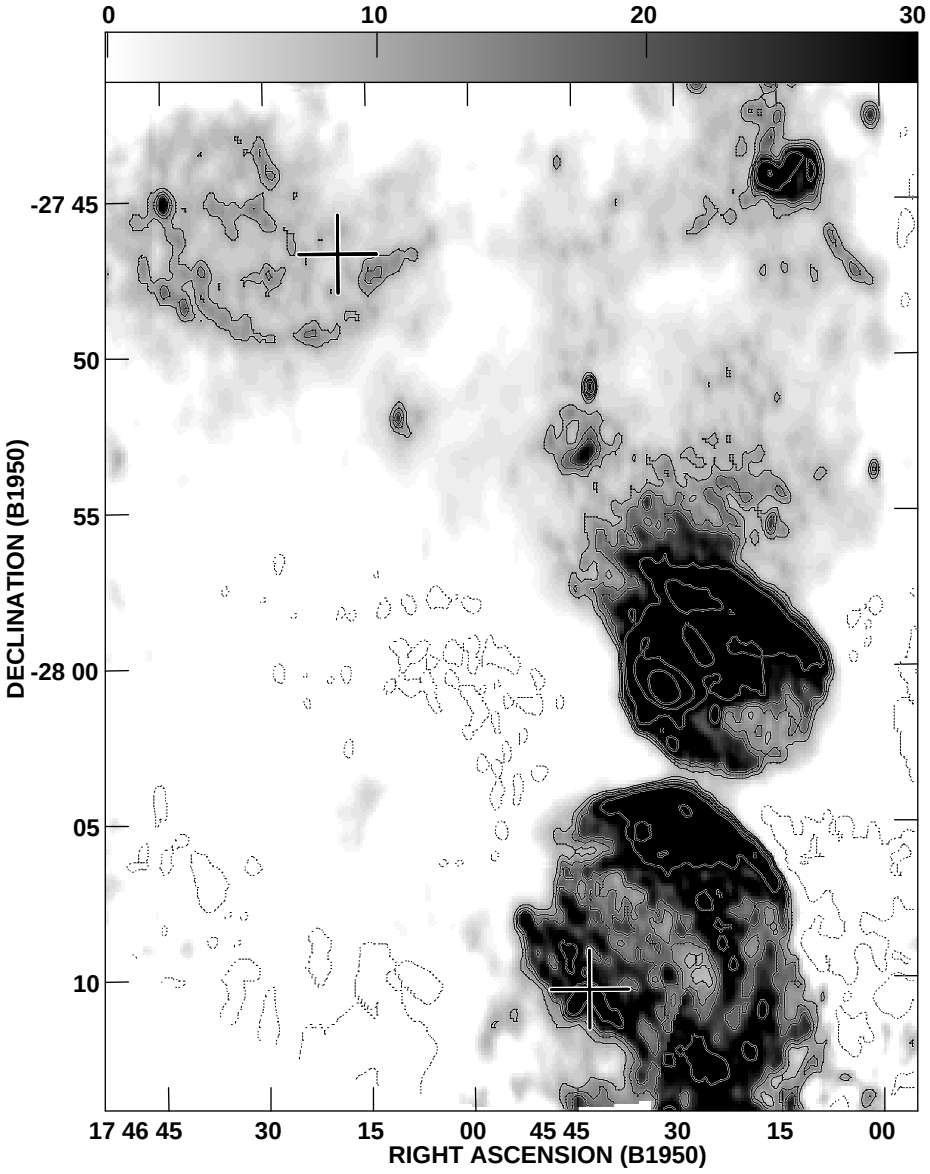

Fig. 5.— A grey-scale continuum mosaic image displayed in black shows prominent thermal source G1.13–0.1 to SW and the nonthermal sources G1.05–0.15 and G1.4–0.1 with a resolution of $30'' \times 15''$ (Liszt 1992) near $\alpha, \delta(1950) = 17^{\rm h}45^{\rm m}30^{\rm s}, -28°08'$ and $17^{\rm h}46^{\rm m}35^{\rm s}, -27°47'$, respectively. Contours of thermal OH(1720 MHz) emission associated with G1.13–0.1 at a velocity of –16.2 $\rm km s^{-1}$ are superposed. The contour levels are 10 × (–3, 3, 4, 5, 6, 7, 8, 9, 11, 13 and 15) mJy $\rm beam^{-1}$. The crosses represent the positions of OH(1720 MHz) maser spots with a resolution of $2\farcs75 \times 1\farcs35$ and an rms noise per channel of 21 mJy $\rm beam^{-1}$.

TABLE 1

GAUSSIAN FITS FOR OH(1720 MHz) MASER FEATURES

Maser Designation	α_{1950} (h m s)	δ_{1950} (° ′ ″)	S_p (Jy)	V_{LSR} (km s^{-1})	ΔV (km s^{-1})	Size major (″)	Size minor (″)	PA (°)
G357.7+0.3 OH1720:A1 (–34)	17 35 17.44±0.01	−30 31 36.8±0.1	0.20±0.02	−34.12±0.02	0.78±0.06	–	–	–
G357.7+0.3 OH1720:A2 (–36)	17 35 18.08±0.01	−30 32 00.6±0.1	0.49±0.03	−35.59±0.01	0.60±0.02	2.7±0.1	1.6±0.1	20±5
G357.7+0.3 OH1720:A3 (–36)	17 35 17.71±0.02	−30 32 07.8±0.3	0.08±0.02	−35.85±0.06	0.78±0.14	4.9±0.6	2.5±0.6	42±12
G357.7+0.3 OH1720:A4 (–37)	17 35 17.47±0.02	−30 32 10.4±0.3	0.08±0.02	−35.75±0.08	1.02±0.18	4.0±0.9	3.1±0.7	21±37
G357.7+0.3 OH1720:A5 (–37)	17 35 16.82±0.01	−30 32 28.2±0.1	0.49±0.02	−37.20±0.01	0.93±0.03	1.5±0.1	0.74±0.1	6±6
G357.7-0.1 OH1720:A1 (–12)	17 36 54.57±0.01	−30 56 07.8±0.1	0.21±0.02	−12.23±0.04	0.95±0.09	2.4±0.5	1.1±0.4	3±15
G1.4-0.1 OH1720:A1 (–2.2)	17 46 19.17±0.01	−27 46 41.3±0.16	0.14±0.02	−2.50±0.01	1.02±0.03	3.1±0.4	0.8±0.4	26±6
G1.4+0.1 OH1720:A2 (–2.5)	17 46 19.11±0.01	−27 46 42.4±0.2	0.10±0.01	−2.31±0.01	1.02±0.10	3.3±0.3	0.9±0.2	20±4
Sgr D OH1720:A1 (–1.4)	17 45 43.15±0.01	−28 10 22.1±0.06	0.30±0.03	−1.38±0.02	0.72±0.04	–	–	–

Fig. 6.— Table 1